Characterisation of Wind-Driven Ventilation in Complex Terrain Conditions

Daniel Micallef, Damien Bounaudet, Robert N. Farrugia, Simon P. Borg, Vincent Buhagiar, Tonio Sant

Abstract—The physical effects of upstream flow obstructions such as vegetation on cross-ventilation phenomena of a building are important for issues such as indoor thermal comfort. Modelling such effects in Computational Fluid Dynamics simulations may also be challenging. The aim of this work is to establish the cross-ventilation jet behaviour in such complex terrain conditions as well as to provide guidelines on the implementation of CFD numerical simulations in order to model complex terrain features such as vegetation in an efficient manner. The methodology consists of onsite measurements on a test cell coupled with numerical simulations. It was found that the cross-ventilation flow is highly turbulent despite the very low velocities encountered internally within the test cells. While no direct measurement of the jet direction was made, the measurements indicate that flow tends to be reversed from the leeward to the windward side. Modelling such a phenomenon proves challenging and is strongly influenced by how vegetation is modelled. A solid vegetation tends to predict better the direction and magnitude of the flow than a porous vegetation approach. A simplified terrain model was also shown to provide good comparisons with observation. The findings have important implications on the study of cross-ventilation in complex terrain conditions since the flow direction does not remain trivial, as with the traditional isolated building case.

Keywords—Complex terrain, cross-ventilation, wind driven ventilation, Computational Fluid Dynamics (CFD), wind resource.

I. INTRODUCTION

THE wind driven cross-ventilation phenomenon has been researched extensively by means of controlled wind tunnel experiments and Computational Fluid Dynamics (CFD) and also coupled building simulation and CFD approaches [1]–[3]. Most of these studies consider the situation of a room in isolation. The influence of upstream flow obstructions, complex terrain and of low wind speed conditions on internal ventilation flows commonly found in built environments has rarely been investigated in a systematic manner, leaving a gap in the scientific literature on this subject.

Cross ventilation has been often utilised extensively as a passive strategy means in reducing the energy demand associated with ventilation and thermal comfort in buildings [4], [5]. An important aspect in using cross ventilation in buildings is of course being able to predict ventilation potential due to design parameters specific for a particular building project which may be building or site dependent. Research on the subject of ventilation has been studied extensively. This includes full CFD numerical investigations studying the opening location in single and cross sided ventilation [6] as well as in depth studies of the expected airflow through

Daniel Micallef is with the University of Malta, Malta (e-mail: dmic0001@gmail.com).

a variety of window openings and typologies [7]. In both cases the authors assumed the building in isolation, with undisturbed air flow approaching the building model. However, as discussed by Shiradzi et al. [1] specifically for the case of cross ventilation in highly packed urban terrains, the authors indicate how flow obstruction has a direct influence on the attained results. Similarly, the case of complex terrain offers a disturbed and turbulent airflow which effects the overall potential of natural ventilation entering an overlooking building aperture.

The motivation behind this work is to address the research questions presented in Section I-A.

A. Aims and Research Questions

It is hypothesised that the cross-flow potential of buildings located in peri-urban sites with upstream vegetation and downstream buildings/structures is non-negligible. The main research question addressed in this paper is: *How does upstream vegetation influence the cross-ventilation rate in a test cell?*. This question is further detailed in two sub questions addressed in this work:

1) What is the direction of the ventilation flow within the test cells?
2) What role does the vegetation porosity have on the prediction of the velocities within the test cell?

In line with the above research questions the aims of this paper are to characterise the wind driven cross-ventilation flow in a test cell located in a complex terrain with upstream vegetation on one side and surrounding buildings on the other. In addition, the sensitivity of the CFD model to the treatment of vegetation as a momentum sink is assessed. The study was carried out using wind flow data which is coming from a northerly direction only to study the simplest case where the wind is perpendicular to the faade opening.

B. Paper Structure

The aims and objectives of the paper are described in the next sub-section. The reader is first introduced to the experimental and numerical approaches used in this study. The results are presented by first considering the measured wind resource on-site using both an ultrasonic and cup anemometer and wind direction vane. A sample of the instantaneous flow velocities within the test cell are presented. Averaging criteria for flow measurements within the test cells are presented and compared with steady state numerical analysis on the basis of a simplified terrain model. These results are then discussed

World Academy of Science, Engineering and Technology
International Journal of Aerospace and Mechanical Engineering
Vol:12, No:3, 2018

and major salient points extracted. The paper concludes with an exposition of the main achievements with this work and on future potential research areas.

II. METHODOLOGY

A. Site Description

The test site is located on the outskirts of the University of Malta campus and is characterised by three rectangular test cells having dimensions of $2.5m \times 2.5m$ plan and $2.2m$ height. The test cells' northern sides overlook a highly vegetated area and a valley having complex topographical features and an urban area further upstream. The vegetation is mainly comprised of indigenous carrob tree (semi-permeable) and prickly pear trees which are practically impermeable. This vegetation is low lying with respect to the three tests cells and are approximately of the same height as the test cells. On the southern side, adjacent buildings are located. Fig. 1 shows the setup in question along with the location of the measuring devices. The westerly cell is used as the measurement test cell since it is the least obstructed by buildings on the southern side. The distance between the measurement cell and the nearest building was 25m. The measurement test cell has two openings facing north and south, allowing for direct cross-ventilation. The openings have the same size of $1.075m \times 1.075m$.
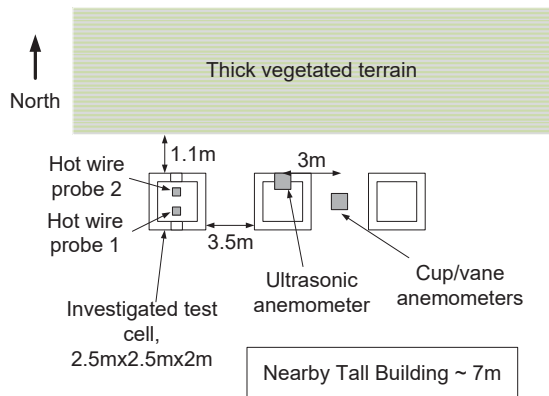

Fig. 1 Top view of setup and critical dimensions.

B. Measurement Campaign

Wind speed and direction measurements are carried out using an ultrasonic anemometer (Thies Clima Ultrasonic Anemometer 3D [8]) located at a height of 5m above ground level (located on top of the central cell) and the mast mounted cup anemometer and direction vane (for model details see [9])is located at 5.5m above ground level in between the central and east cells (see Fig. 1). The data collected were synchronised to a common time stamp and checked. A directional filtering process was conducted in order to only consider records for winds blowing towards the test site from the North (for direction angle greater than 350° and less than

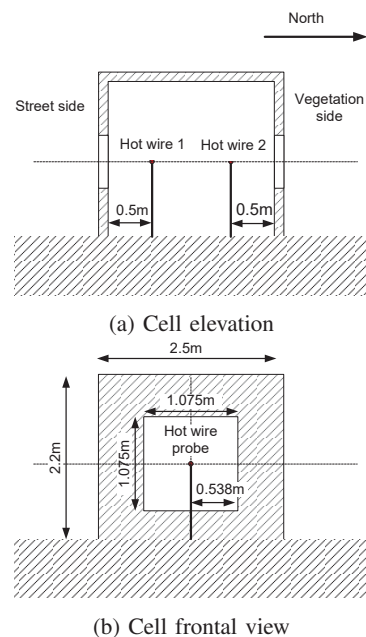(a) Cell elevation

(b) Cell frontal view

Fig. 2 Cell dimensions and hot wire positions

10°); thus eliminating the influences of flow past the adjacent test cells and of buildings and other obstacles in all other sectors.

C. Test Cell Velocity Measurements

Velocities within the measurement test cell are carried out at two points using constant temperature hot wire anemometry (Kimo VT110) directly synchronised with the ultrasonic and cup/vane anemometers. Sampling frequencies varied from 1Hz to 0.2Hz depending on the data logger storage limitations. The hot wire probes were located at the centre of the cell openings but at a distance of 0.5m away from them (refer to 2 for cell setups). These distances were chosen for the purpose of CFD validation in order to be able to measure and correlate the jet velocity dip commonly reported in literature [2], [10], [11].

D. Limitations of the Experimental Approach

There are three main limitations with the measurements being carried out. The first being the relatively small heights of the ultrasonic and cup anemometers above ground level. The limitation is due to the wind masts available. The measurements being carried out are at least 3m above the vegetation line but still some influence is expected due to the flow blockage caused by the vegetation. This factor is however accounted for within the CFD approach described in Section II-E.

A second limitation is that testing was conducted during the summer months when wind speeds are low and also that the sectorial filtering for northerly winds limits the number of data points captured given that the prevailing winds in Malta are the north westerlies. Both of these limitations were unavoidable for the campaign programme envisaged in this work.

The third main limitation is the uncertainty in the hot-wire measurements at low flow velocities. Velocities lower than

World Academy of Science, Engineering and Technology
International Journal of Aerospace and Mechanical Engineering
Vol:12, No:3, 2018

0.15m/s cannot be measured reliably due to the predominating effect of natural convection. Also, the probe orientation relative to the flow needs to also be perpendicular to the main flow direction as much as possible. This is not easily attainable given that the jet tends to exhibit a slight downward or upward shift depending on the direction of the jet. The uncertainty in the measurement due to an error in orientation is found to be 4.49%. The full uncertainty analysis is based on the calculation of the orientation error $\Delta\Theta$ as calculated from the CFD simulations.

The percentage uncertainties as a result of the probe orientation relative to the flow direction is estimated from the numerical simulations in order to give an indication of this possible issue with the experimental data. According to Jørgensen [12] the uncertainty due to the probe orientation is given by:

$$U = \frac{1}{\sqrt{3}}\left(1 - cos\Delta\Theta\right) \qquad (1)$$

where $\Delta\Theta$ corresponds to the flow angle orientation with respect to the horizontal axis:

$$\Delta\Theta = tan^{-1}\left(\frac{V_y^0}{V_x^0}\right) \qquad (2)$$

where V_x^0 and V_y^0 are the x and y velocities at the probe position. The velocity vectors obtained from simulation at a cross section of the flow within the test cell are shown in Fig. 3 for the case of 5m/s reference wind speed. The positions of the hot wires are also indicated. As will be discussed in the results section, the flow is strongly effected by the way the vegetation is modelled. In Tables I and II, these uncertainties are shown. For the solid vegetation case (which was found to more reliably model the test cell velocities), the maximum uncertainty is found on hot wire 1 with a percentage of 4.49%.

TABLE I Uncertainty in probe orientation for the solid vegetation case.

Case	5m/s	Solid vegetation		
	V_x	V_y	$\Delta\Theta$	% uncertainty
Hot wire 1	-0.6086	0.255	22.73	4.49
Hot wire 2	-0.2893	-0.0088	1.74	0.03

TABLE II Uncertainty in probe orientation for the porous vegetation case

Case	5m/s	Porous vegetation		
	V_x	V_y	$\Delta\Theta$	% uncertainty
Hot wire 1	0.3633	-0.0144	2.27	0.05
Hot wire 2	0.6787	-0.3734	28.82	7.15

E. CFD Model

In order to address one of the research questions in this project, a simplified geometrical model of the site is being proposed in order to assess the effects of these simplifications on the results. Two methodologies for vegetation modelling are considered (i) where vegetation is modelled to produce a finite drag on the flow and hence producing a momentum sink and (ii) where the vegetation is modelled as a solid block. These two approaches will be further described in this
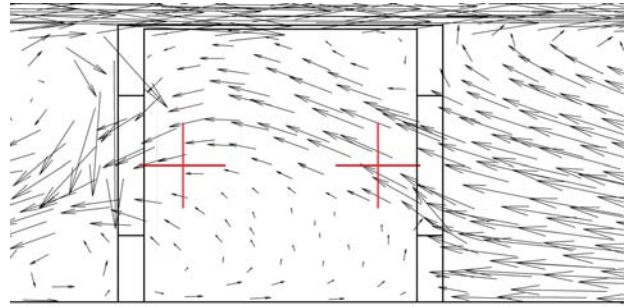

Fig. 3 Velocity vectors indicating flow directions. Left cross-hair indicates hot wire 2 while right cross-hair indicates hot wire 1. The case shown here is for solid vegetation at a 5m/s reference wind speed

section. The model was implemented in the commercial code ANSYS®Fluent [13]. Topographic variations in the upstream stretch of land is ignored and the vegetation is treated as a block measuring 26m long by 2.2m high. The effect of the downstream buildings is also ignored although this is not expected to have a major effect on the flows within the test cell due to the large distance (≈ 12.5 times the test cell dimension) between the two. The size of the domain used is in line with established guidelines in [14], [15] measuring 69.2m long, 38.5m wide and 15.4m high. The geometry of the domain and boundary conditions are shown in Fig. 4. The inlet boundary condition is prescribed as a power law profile as follows:

$$\frac{U(y)}{U_A} = \left(\frac{y}{H_A}\right)^{\alpha} \qquad (3)$$

where $U(y)$ is the wind velocity at a height y from ground level, U_A is the mean wind speed measured at the anemometer height, H_A is the anemometer height and α is the power law exponent taken as 0.2 in accordance with the European Wind Atlas roughness definitions [16]. A uniform turbulence intensity at the inlet is assumed corresponding to the turbulence intensity measured by the Ultrasonic anemometer. The outlet is prescribed as a pressure outlet.

The efforts made to simplify the geometry of the model have the advantage of enabling a structured mesh making it easier to ensure mesh quality compared to an unstructured approach.
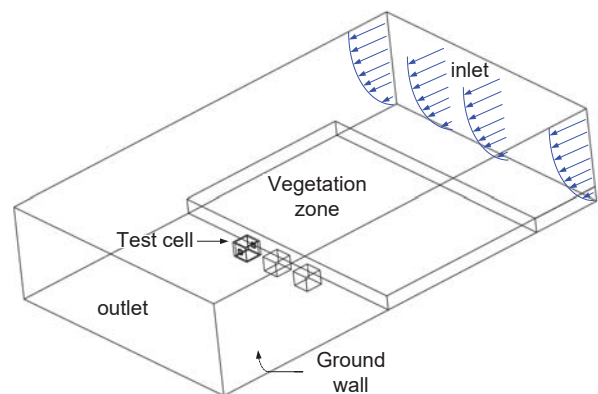

Fig. 4 Geometry of the model with boundary conditions shown. Side walls and top 'lid' are prescribed as symmetry boundary conditions

World Academy of Science, Engineering and Technology
International Journal of Aerospace and Mechanical Engineering
Vol:12, No:3, 2018

The CFD model numerically solves the continuity and momentum equations as described in [17]. These equations are shown hereunder with respectively with the momentum equation only shown for the x direction corresponding to the wind direction

$$\nabla \cdot \mathbf{u} = 0 \qquad (4)$$

$$\nabla \cdot (\rho u \mathbf{u}) = -\frac{\partial p}{\partial x} + \nabla \cdot (\mu \nabla \mathbf{u}) + \underbrace{S_x(x,y,z)}_{\text{vegetation drag}} \qquad (5)$$

Where $\mathbf{u}$ is the velocity vector, u is the velocity in the x direction, ρ is the density, p is the pressure and μ is the viscosity. The cartesian coordinates are x, y, z. $\nabla\cdot$ is the divergence operator while ∇ is the *grad* operator.

F. Vegetation Modelled as Finite Momentum Sink

The vegetation zone shown in Fig. 4 is modelled using a body force function indicated in (5) as $S_x(x,y,z)$ in N/m^3. The body force is assumed to be one-dimensional with $S_y(x,y,z) = S_z(x,y,z) = 0$. The vegetation body force function supposedly varies with the vegetation morphology but here, the whole vegetation block is assumed to cause the same force per unit volume and is hence made independent of position. From here onwards this term will be concisely referred to simply as S_x. Fig. 5 shows how the vegetation drag is treated for a particular cell within the vegetation zone indicated in Fig. 4. The air is slowed down due to the drag force imposed on the air flowing through the cell.
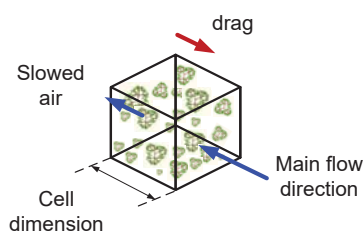

Fig. 5 Drag force acting on each vegetation cell. This is used to calculate the source term S_x

The drag force acting on the cell is given by:

$$D = \iiint_V S_x dV \qquad (6)$$

The pressure drag on vegetation has been studied in various works such as [18]. Of particular interest is the work of Gromke [19] who tested various tree crowns having different porosities for application at different length scales using similarity arguments. This is used as the primary reference for specifying the body forces caused by the vegetation. In this case, due to the large fetch of vegetation upstream of the test cell, the flow velocities on each adjacent cell in the downstream direction will be largely slowed down resulting in very low Re flows. Data for the pressure drop at such low Re numbers is unavailable not only in the work of Gromke [19] but also in other works studying the drag caused by

various vegetation types including that from Manickathan et al. [18] who give drag coefficient for entire trees (including trunk). Grunert [20] provide various values for λ for different shelterbelt types which vary from $0.4 m^{-1}$ up to $13.4 m^{-1}$. In the present work, the loss coefficient is represented as the drag coefficient per unit cell length. The work of Manickathan [18] is used as reference for determining C_d. The tree species considered by the authors are not the same as those found on the current site but the foliage is rather similar. The site is characterised by Prunus dulcis, syn. Prunus amygdalus - bitter almond Ceratonia siliqua - Carob which are considered to be very similar to one of the models tested by Manickathan et al. [18]. The data of these authors is fit to a second order polynomial of Re number as given in (7). The following conditions are used:

$$C_D(\text{Re}) = \begin{cases} 0.8 & \text{if } Re \leq 10^3 \\ 10^{-19}\,\text{Re}^2 -3 \times 10^{-10}\,\text{Re} \\ \quad +0.8303 & \text{if } 10^3 < \text{Re} \leq 10^9 \\ 0.67 & \text{if } \text{Re} > 10^9 \end{cases} \qquad (7)$$

The source term is then found from (7) and the resulting formula is:

$$S_x = \frac{\frac{1}{2}\rho u^2 C_D}{\Delta x} \qquad (8)$$

where u is the local flow velocity, Δx is the cell dimension along the wind flow direction.

It must be appreciated that the velocities at each cell within the vegetation will be low and hence most C_d values will correspond to an assumed 0.8 at low Re. This is most probably an underestimation, but with the current available data no improvements can be made. For better stability of the solution it was also found better to relax the magnitude of this drag coefficient and therefore to slow down the air gradually rather than abruptly as it flows through the vegetation zone.

G. Vegetation as a Solid Block

The second approach considered is to model thick vegetation present on site as a solid block. This is clearly an unphysical assumption but could actually result in better flow prediction approach than the previously mentioned drag approach. This hypothesis is tested within research question number two specified in Section I-A.

H. Solver Details

Turbulence closure is performed by means of a RANS approach using Renormalization Group (RNG) $k - \epsilon$ model [21] given its success in previous research to solve problems involving high flow separation and for cross-ventilation problems [22]. This turbulence model was designed to cater for high Re flows. In [2] on the basis of the experimental data found in [23], it is argued that the SST $k - \omega$ model is able to better predict the cross-ventilation flows inside a cubic building. This conclusion could also be tested in the context of this work but is left for future work.
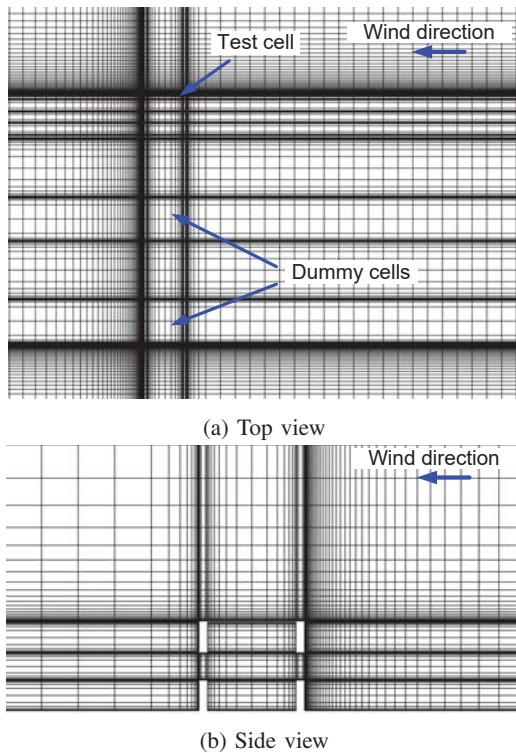
World Academy of Science, Engineering and Technology
International Journal of Aerospace and Mechanical Engineering
Vol:12, No:3, 2018

(a) Top view

(b) Side view

Fig. 6 Mesh details close to the test cell

I. Verification

Mesh independence was tested using the Grid Convergence Index (GCI) approach proposed by Roache [27], [28]. Three grids were used of 600 thousand, 900 thousand and 1.9 million cells for the case of a solid vegetation. The GCI for the velocities measured at the sensor locations was found for a wind velocity corresponding to 5m/s resulting in a GCI of less than 4%. The fine mesh of 1.9 million cells was therefore used as this was considered sufficient to ensure mesh independence while still maintaining acceptable computational times to run a number of simulations. The details of the mesh are shown in Fig. 6.

A limitation of the RNG $k = \epsilon$ model is that some regions of the flow can be associated with low to transitional Res and hence the results could be somewhat impaired. To maintain focus, the sensitivity of results to the turbulence model is not treated here. Wall boundary layers handled using the enhanced wall treatment (see [13], [24]–[26]) wherein, mesh resolved regions ($y^+ < 1$) are solved up to the wall whereas wall regions with $30 < y^+ < 500$ are solved using a wall function approach.

III. RESULTS

A. Wind Statistics

As stated in the aims of the paper, the study is focused on wind coming from a northerly direction (perpendicular to the inlet and outlet opening faades. Fig. 7 shows the wind rose data gathered during the campaign plotted in the form of a wind rose plot. The wind rose shows the data frequency for different

directions. Not surprisingly, most of the data measured comes from the Northwest and they are also the strongest. This is known to be the annual statistically prevailing wind direction in Malta. This data comes from the cup anemometer, which is taken as the reference data (the ultrasonic anemometer data is actually very similar to the cup anemometer even though its around 0.5m lower in terms of height). The strong influence of the building present to the south of the cells is also clear with only extremely small number of events from this direction. Unfortunately only 3% of the data is associated with Northerly winds and this is further subdivided into bins of different velocities. For the purpose of correlating the wind speed data with the in-cell hotwire measurements this is considered to be adequate as shall be shown in the analysis which follows.
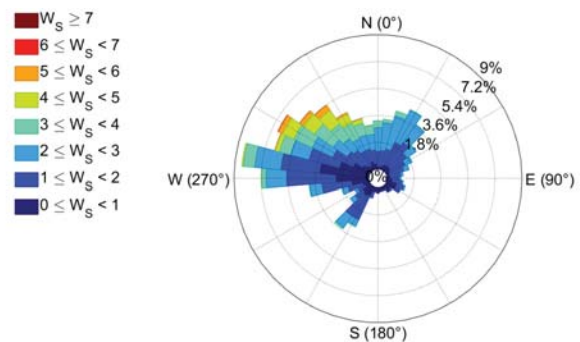

Fig. 7 Wind rose for the site after 3 months of data gathering

The difference in the readings obtained between the ultrasonic and cup/vane anemometers is better shown by means of a scatter plot. Fig. 8 shows a plot of ultrasonic anemometer measured velocity against that obtained from the cup anemometer. The data has an R^2 value of 0.79. The deviation from $R^2 = 1$ is associated with the 0.5m difference in height and the 3m lateral distance of separation between the two anemometers. This scatter is also attributable in part to the turbulence present on site.
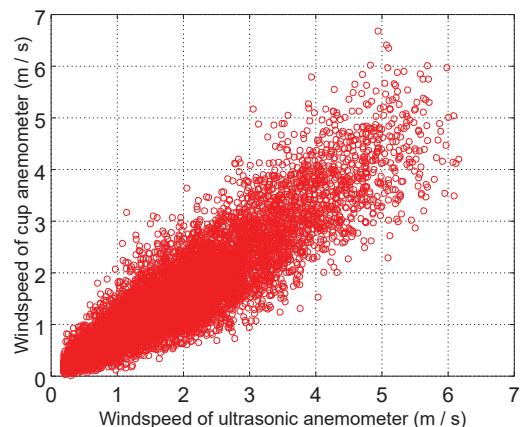

Fig. 8 Comparison of the ultrasonic and cup anemometer wind velocity results

As previously indicated in order to be able to investigate the wind coming from the northern sector, data is binned

World Academy of Science, Engineering and Technology
International Journal of Aerospace and Mechanical Engineering
Vol:12, No:3, 2018

within $\pm 10°$ of the true north direction to account for data uncertainty.

B. Correlation between Wind Speed and Indoor Velocities

A check for any particular correlation between the indoor velocities and the external wind speed is made here. The ultrasonic anemometer data is used as reference. The reason for this is that it is located closer to the test cell of interest despite being at a slightly lower height than the cup anemometer. A sample of the data is plotted in Fig. 9 with the hotwire measurements for the two probes on the vertical axis and the ultrasonic wind speed measurements on the horizontal axis. This data is for winds coming from a northern sector.

It is clear that the data coming only from both hot wires is very sparse with most cell velocities falling below 0.5m/s. Turbulence plays a major role in explaining the kind of data scatter observed in these plots. The high velocity data points which in some cases exceed 1m/s can be associated with turbulent structures of length scale equal to or smaller than the window openings. It is interesting to note that the data measured by both probes has a similar scatter but for hot wire probe 2, the measured velocities are somewhat smaller than those observed by hot wire 1. Given that hot wires do not provide any information on the flow direction the data itself does not give direct information on the jet orientation. Nonetheless, the observed differences in velocities between the hot wire measurements can be an indication that the jet enters from the leeward side of the cell and not from the windward side. The lower velocities measured by hotwire 2 is an indication of the jet turbulence dissipation. This hypothesis needs to be confirmed by means of the numerical simulations which will be presented later.

C. Test Cell Flows

In order to compare mean velocities within the test cell, data is plotted for the average hot wire measurements against the various wind speeds. The wind speed data for the northern sector is this time taken from the cup anemometer since this is at the highest location. The data is further binned corresponding to wind speeds of $U_\infty = \{0.25, 1, 2, 3, 4, 5\} m/s$ within the range $\pm 0.5 m/s$. The hot wire measurements corresponding to each of these mean wind speeds are averaged out. This allowed for a direct comparison with the steady state simulations carried out over the range of wind speeds considered. The standard deviation is plotted in the form of error bars in order to be able to visualise the scatter of the data about the mean. The lower error bar is clipped at 0m/s since the velocity magnitude cannot be negative. Due to the characteristics of this data, the purpose of this validation study is limited to indicating the trend of the mean velocities as well as the order of magnitude of such velocities. Large eddy simulation capable of resolving turbulent length scales found within the room are necessary in order to be able to also quantify the validity of the data scatter.

The measurements are compared with two cases where the vegetation is modelled in accordance with drag approximations

(a) Hot wire 1 velocity against wind speed
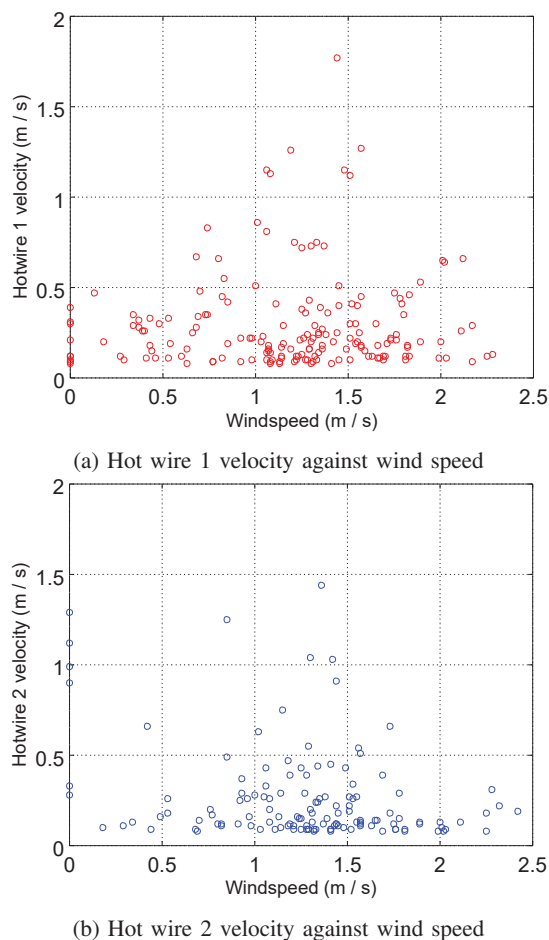

(b) Hot wire 2 velocity against wind speed

Fig. 9 Hot wire measurements against wind speed for northern sector winds(perpendicular to the test cell face) as obtained from the ultrasonic anemometer. The north wind direction uncertainty was binned on the basis of $\pm 10°$ uncertainty range. Data is 1 minute averaged

governed by (7) and the case where the vegetation acts as a solid with zero porosity.

Fig. 10 shows the velocities as measured by hot wire 1 against the averaged wind speeds both as measured as well as the computed velocities by means of the CFD model using the porous and solid vegetation models. The CFD data in both types of vegetation models is in acceptably good agreement. For the porous approach in modelling vegetation the data agrees well for lower wind speeds of 1m/s, 2m/s and 3m/s. At the higher wind speeds of 4m/s and 5m/s some deviations arise. With the solid vegetation model, the data shows very good agreement over all wind speeds considered. Fig. 11 plots the same variables but for the position of hot wire 2 (which is facing the vegetation). The velocity as calculated using the porous vegetation model deviates significantly from experiment. Most importantly it is noticed that the velocities are higher than for hot wire 1 which means that the direction of the jet is from the windward to the leeward side (this was also confirmed when only the x velocities where checked). The velocity magnitude calculations with the solid vegetation model provides much better agreement with the experimental data. In this case, in line with what is observed with the on-site

World Academy of Science, Engineering and Technology
International Journal of Aerospace and Mechanical Engineering
Vol:12, No:3, 2018

measurements, the magnitude of the velocity at hot wire 2 is smaller than that from hot wire 1 indicating that the jet direction is predominantly from the leeward to the wind ward side. This is well predicted with the solid vegetation model.

Fig. 12 gives results for turbulence intensity against wind speed measured at the ultrasonic anemometer position. An attempt was made to modify the uniform turbulence intensity at the inlet to domain but the results from both the porous and solid vegetation model were both still off from the experimental measurements particularly in the higher wind speed range. The results shown in the figure correspond to the case when the inlet was maintained at 35%. As can be seen, the results are under-predicted for low wind speed and over-predicted for higher wind speeds. The reason for this is mostly associated with the RANS approach used which is known to be problematic in regions of high separation with over-prediction of the turbulent kinetic energy.
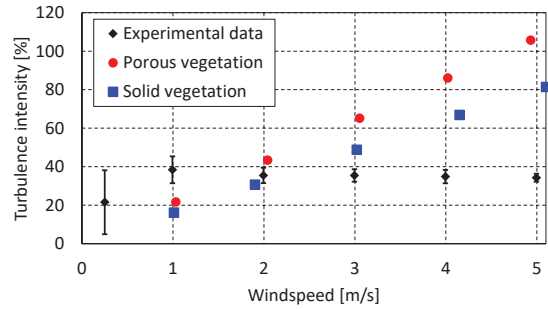

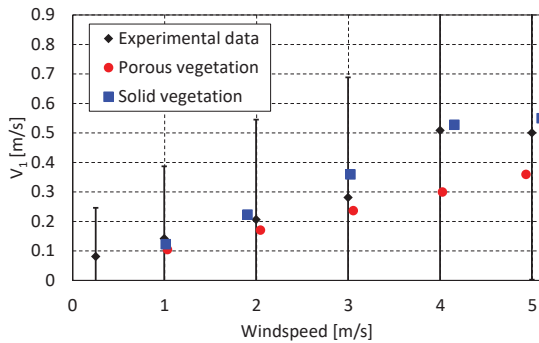Fig. 12 Turbulence intensity against wind speed at the cup anemometer location

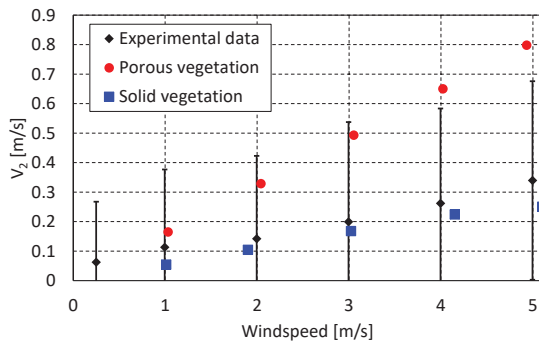Fig. 10 Velocity at the position of hot wire 1 against averaged wind speed

Fig. 11 Velocity at the position of hot wire 2 against averaged wind speed

D. Window Jet Physics: Effects of Upstream Vegetation

From the previous results it is clear that the porosity and drag characteristics have a substantial role to play in the jet physics coming from the window. Fig. 13 shows the x velocity when the vegetation is modelled by a finite momentum sink (7). Fig.14 is the case when the vegetation is modelled as a zero porosity block. In both cases, the colorbar is clipped to $\pm 1.5 m/s$ so that velocities outside this range are not coloured. This helps to visualise the flow within the test cells better. The wind speed, is shown as an arrow from left to right. When

vegetation is modelled as a drag, the window jet is diverted downwards as a result of the flow direction just upstream of the cell. The role of the drag forces are basically to slow down the air upstream but the approach velocity on the wind ward window is still from left to right. This, in combination with a vertical downward flow from the building faade causes this downward direction of the jet. The case where the vegetation acts as a solid shows that the flow direction through the cell is from right to left i.e. opposite to the main flow direction. As a result of the clockwise circulating flow behind the cell, the jet flow direction is this time oriented upward towards the cell ceiling.
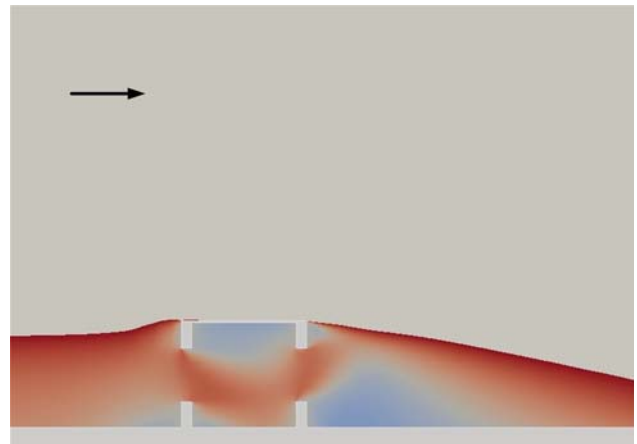

Fig. 13 Velocity in the x direction when vegetation is modelled as a drag force. Wind speed at the reference height is 5m/s. The colour bar is clipped at $\pm 1.5 m/s$ for clarity

IV. DISCUSSION

The difference between the velocities at the hot wire positions as measured and as calculated when using the drag of (7) (porous approach) is an indication that the model is not correctly predicting the direction of the jet given the difference in velocities between hot wire 1 and hot wire 2. This observation is confirmed when using a solid vegetation model with the resulting effect that hot wire 1 now reads a higher velocity than hot wire 2, consistent with what is observed. A solid/thick vegetation causes a region of strong underpressure in the area between the vegetation and the cell.

World Academy of Science, Engineering and Technology
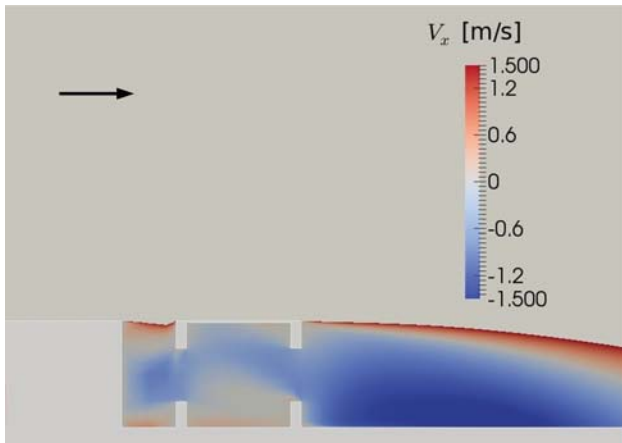International Journal of Aerospace and Mechanical Engineering
Vol:12, No:3, 2018

Fig. 14 Velocity in the x direction when vegetation is modelled as a solid block. Wind speed at the reference height is 5m/s. The colour bar is clipped at $\pm 1.5 m/s$ for clarity

This underpressure depression on the wind-ward façade is even larger than the under pressure resulting on the lee-ward façade of the cell causing flow reversal from the road side towards the vegetation side. This has practical implications such as in the context of pollution dispersal as well as thermal conditions within the test cell. For instance, if one where to consider the influence of evapo-transpiration on the thermal performance of the test cell, the current results indicate that the flow is not directed from the vegetation side towards the cell but the other way round causing a different convection physics of humidity. In terms of modelling, thick vegetation seems to resemble more the case of a solid region with zero porosity but is highly dependent on the type of vegetation. Optimisation of this result to account for the finite porosity of the vegetation would be necessary but is not considered here.

Again it must be stressed that the uncertainties of the experimental data measured need to be kept in mind when interpreting this data and the fact that the numerical data falls within the error bars is encouraging given the site complexity. Certainly in terms of modelling approach, the way the porosity of the upstream vegetation plays a fundamental role in the prediction of the flow within the test cell. The effects of surrounding buildings can also be non-negligible on the pressures found on the lee-ward façade despite the fact that these are located more than twelve times the test cell height.

V. CONCLUSIONS

The following conclusions can be drawn from this work:

- There is substantial scatter between the wind velocity data on site and the velocities internal to the test cell measured by the hotwires. This is attributed to the strong turbulence effects still prevalent even for the small velocities encountered within the test cells.
- The porosity of upstream vegetation is modelled as a drag force on the flow causing (finite momentum sink) and a solid block (infinite momentum sink).
- It is found that the porosity of the upstream vegetation has a crucial role to play on the jet physics from the openings.

- A thick/solid upstream vegetation causes a cross-ventilation reversal flow from the lee-ward to the wind-ward side of the test cell.
- A finite momentum sink vegetation model with the drag modelled with (7) results in a traditional cross-flow direction from the wind-ward to the lee-ward side of the building.
- From the averaged site measurements it transpires that in this case the vegetation acts more like a solid zone given the thick vegetation found on site.

REFERENCES

[1] M. Shirzadi, M. Naghashzadegan, and P. A. Mirzaei, "Improving the CFD modelling of cross-ventilation in highly-packed urban areas," *Sustainable Cities and Society*, vol. 37, pp. 451–465, 2018. (Online). Available: http://www.sciencedirect.com/science/article/pii/S2210670717312891.

[2] R. Ramponi and B. Blocken, "CFD simulation of cross-ventilation for a generic isolated building: Impact of computational parameters," *Building and Environment*, vol. 53, pp. 34–48, jul 2012. (Online). Available: http://www.sciencedirect.com/science/article/pii/S0360132312000133.

[3] L. Wang and N. H. Wong, "Coupled simulations for naturally ventilated rooms between building simulation (BS) and computational fluid dynamics (CFD) for better prediction of indoor thermal environment," *Building and Environment*, vol. 44, no. 1, pp. 95–112, jan 2009. (Online). Available: http://www.sciencedirect.com/science/article/pii/S0360132308000231.

[4] A. H. Abdullah and F. Wang, "Design and low energy ventilation solutions for atria in the tropics," *Sustainable Cities and Society*, vol. 2, no. 1, pp. 8–28, 2012. (Online). Available: http://www.sciencedirect.com/science/article/pii/S2210670711000606.

[5] A. Mochida, H. Yoshino, S. Miyauchi, and T. Mitamura, "Total analysis of cooling effects of cross-ventilation affected by microclimate around a building," *Solar Energy*, vol. 80, no. 4, pp. 371–382, 2006. (Online). Available: http://www.sciencedirect.com/science/article/pii/S0038092X05003075.

[6] X.-Y. Ma, Y. Peng, F.-Y. Zhao, C.-W. Liu, and S.-J. Mei, "Full Numerical Investigations on the Wind Driven Natural Ventilation: Cross Ventilation and Single-sided Ventilation," *Procedia Engineering*, vol. 205, pp. 3797–3803, 2017. (Online). Available: http://www.sciencedirect.com/science/article/pii/S1877705817346842.

[7] H. Wang, P. Karava, and Q. Chen, "Development of simple semiempirical models for calculating airflow through hopper, awning, and casement windows for single-sided natural ventilation," *Energy and Buildings*, vol. 96, pp. 373–384, 2015. (Online). Available: http://www.sciencedirect.com/science/article/pii/S0378778815002509.

[8] T. Clima, "Ultrasonic anemometer 3D operating instructions," Tech. Rep., 2012. (Online). Available: http://www.novalynx.com/images/200-81000.jpg.

[9] W. Ltd., "www.windspeed.co.uk." (Online). Available: www.windspeed.co.uk.

[10] T. van Hooff, B. Blocken, and Y. Tominaga, "On the accuracy of CFD simulations of cross-ventilation flows for a generic isolated building: Comparison of RANS, LES and experiments," *Building and Environment*, vol. 114, pp. 148–165, 2016. (Online). Available: http://linkinghub.elsevier.com/retrieve/pii/S036013231630511X.

[11] D. Micallef, V. Buhagiar, and S. P. Borg, "Cross-ventilation of a room in a courtyard building," *Energy and Buildings*, vol. 133, pp. 658–669, 2016. (Online). Available: http://linkinghub.elsevier.com/retrieve/pii/S0378778816309124.

[12] F. Jørgensen, "How to measure turbulence with hot-wire anemometersa practical guide," *Dantec Dynamics*, p. 3244, 2002.

[13] I. Ansys, "ANSYS Fluent Theory Guide," vol. 15317, no. November, p. 514, 2013.

World Academy of Science, Engineering and Technology
International Journal of Aerospace and Mechanical Engineering
Vol:12, No:3, 2018

[14] B. C. Jörg Franke, Antti Hellsten, Heinke Schlünzen, *Best Practice Guideline for the Cfd Simulation of Flows in the Urban Environment Quality Assurance and Improvement of*, 2007, no. May.

[15] Y. Tominaga, A. Mochida, R. Yoshie, H. Kataoka, T. Nozu, M. Yoshikawa, and T. Shirasawa, "AIJ guidelines for practical applications of CFD to pedestrian wind environment around buildings," *Journal of Wind Engineering and Industrial Aerodynamics*, vol. 96, no. 10-11, pp. 1749–1761, oct 2008. (Online). Available: http://www.sciencedirect.com/science/article/pii/S0167610508000445.

[16] M. Ray, A. Rogers, and J. McGowan, "Analysis of Wind Shear Models and Trends in Different Terrains," *AWEA Wind Power 2005 Conference*, no. June 2006, pp. 4–7, 2006.

[17] H. K. Versteeg and W. Malalasekera, *An Introduction to Computational Fluid Dynamics: The Finite Volume Method*. Pearson Education Limited, 2007. (Online). Available: http://books.google.com.mt/books?id=RvBZ-UMpGzIC.

[18] L. Manickathan, T. Defraeye, J. Allegrini, D. Derome, and J. Carmeliet, "Aerodynamic characterisation of model vegetation by wind tunnel experiments," no. June, pp. 30–31, 2016.

[19] C. Gromke, "Modeling vegetation in Wind Engineering wind tunnel studies," *The Seventh International Colloquium on Bluff Body Aerodynamics and Applications*, pp. 1421–1428, 2012.

[20] K. Grunert, F., Benndorf, D., Klingbeil, "Neuere Ergebnisse zum Aufbau von Schutzpflanzungen," in *Beiträge für die Forstwissenschaft 18*, 1984, pp. 108–115.

[21] V. Yakhot, S. A. Orszag, S. Thangam, T. B. Gatski, and C. G. Speziale, "Development of turbulence models for shear flows by a double expansion technique," *Physics of Fluids A: Fluid Dynamics (1989-1993)*, vol. 4, no. 7, 1992.

[22] G. Evola and V. Popov, "Computational analysis of wind driven natural ventilation in buildings," *Energy and Buildings*, vol. 38, no. 5, pp. 491–501, may 2006. (Online). Available: http://www.sciencedirect.com/science/article/pii/S0378778805001702.

[23] P. Karava, T. Stathopoulos, and A. K. Athienitis, "Airflow assessment in cross-ventilated buildings with operable façade elements," *Building and Environment*, vol. 46, no. 1, pp. 266–279, 2011.

[24] B. A. Kader, "Temperature and concentration profiles in fully turbulent boundary layers," *International Journal of Heat and Mass Transfer*, vol. 24, no. 9, pp. 1541–1544, 1981. (Online). Available: http://www.sciencedirect.com/science/article/pii/0017931081902209.

[25] H. C. CHEN and V. C. PATEL, "Near-wall turbulence models for complex flows including separation," *AIAA Journal*, vol. 26, no. 6, pp. 641–648, jun 1988. (Online). Available: https://doi.org/10.2514/3.9948.

[26] M. Wolfshtein, "The velocity and temperature distribution in one-dimensional flow with turbulence augmentation and pressure gradient," *International Journal of Heat and Mass Transfer*, vol. 12, no. 3, pp. 301–318, 1969. (Online). Available: http://www.sciencedirect.com/science/article/pii/001793106990012X.

[27] P. J. Roache, K. N. Ghia, and F. M. White, "Editorial Policy Statement on the Control of Numerical Accuracy," *Journal of Fluids Engineering*, vol. 108, no. 1, p. 1, 1986.

[28] P. J. Roache, "Verification and Validation in Computational Science and Engineering." Hermosa Publishers, 1998, pp. 107–141.

Vincent Buhagiar Department of Environmental Design, University of Malta

Tonio Sant Department of Mechanical Engineering, University of Malta

Daniel Micallef Department of Environmental Design University of Malta

Damien Bounaudet University of Nantes, Laboratoire de Thermique et Energie de Nantes

Robert N. Farrugia Institute for Sustainable Energy, University of Malta

Simon P. Borg Department of Environmental Design, University of Malta